A Low-Noise Reconfigurable Full-Duplex Front-End with Self-Interference Cancellation and Harmonic-Rejection Power Amplifier for Low Power Radio Applications

Tong Zhang[1], Yongdong Chen[1], Chenxi Huang[1], and Jacques C. Rudell[1]
Email: togzhang@uw.edu yongdong@uw.edu chenxh@uw.edu jcrudell@uw.edu
[1]Department of Electrical Engineering, University of Washington, Seattle, WA, USA

Abstract— **A low-power radio analog front-end which includes a self-interference (SI) cancellation circuit and a harmonic-rejection power amplifier (HRPA), is proposed to reduce the interaction between a transmitter (TX) and receiver (RX), to enable full-duplex operation. A prototype TSMC device demonstrates more than 30dB SI cancellation over a 4MHz BW and a PA 3rd and 5th harmonic reduction of 30dB and 15dB, respectively. The SI cancellation circuitry occupies an active area of 131×112.5μm², consumes 0.25mW from a 1.2V supply and degrades the RX NF by less than 0.6dB.**

Keywords—Interference Cancellation, CMOS Integrated Circuits, Radio frequency, Radio spectrum management.

I. Introduction

The RF spectrum (100MHz – 6GHz) at present is completely occupied by commercial standards (cellular, WiFi, Bluetooth, etc) along with radio applications that include military and emergency services. This combined with an acceleration in consumer trends toward more wireless network capacity and higher data rates, has motivated researchers to explore more spectral-efficient wireless communication systems, capable of simultaneously transmitting and receiving, using either closely spaced channels, or in the extreme case, the same carrier frequency (full-duplex) [1]–[5]. Full-duplex (FD) communication has the primary advantage of releasing spectrum that would otherwise be exclusively dedicated to either transmitting or receiving. If a single user simultaneously operates both TX and RX, using the same channel frequency, this to first order doubles the spectral efficiency. However, a major challenge with FD radios is the coupling of a single user's TX signal into its own RX. This undesired TX-to-RX self-interference (SI) signal will degrade the RX carrier-to-interference (C/I) ratio, and in the extreme case, saturate the RX. Therefore, attenuation of the TX SI signal as early in the RX chain as possible becomes paramount, to relax the linearity requirements of the low-noise amplifier and RX chain subsequent components [6].

Numerous efforts have explored methods to attenuate a TX leakage carrier signal using passive [6], [7] or active techniques[1], [3], [5]. Active cancelers [1], [3], [5], [8] are challenged from a noise and power perspective, while passive techniques [6], [7] consume more area and result in narrowband solutions.

Switch-mode power amplifiers are widely used in RF systems to achieve high efficiency. The non-linear nature of a switch-mode power amplifier (PA) inherently generates harmonic spurious output, which requires discrete off-chip components to filter unwanted TX spurious output. Conduction angle calibration [9], [10] and passive filters [11] have been reported for harmonic suppression. However, these methods significantly increase the TX insertion loss and require extra chip or board area to accommodate additional components. While all of the aforementioned methods target suppressing the TX self-interference about the carrier frequency, none to date, have sufficient SI cancellation BW to attenuate the residual TX harmonics which also leak to the receiver input.

This paper describes two circuit-level techniques which contribute toward reducing the interaction between the TX and RX, to eventually allow FD operation for low-power compact Bluetooth-like radio applications. In a typical low-power Bluetooth radio, the RX sensitivity is -80dBm and the PA output power is 0dBm. Thus, the TX leakage needs attenuation in the analog/RF and digital domains by more than 90 dB to maintain a sufficient back-end RX SNR, while both receiving a signal at the sensitivity level and the TX is delivering maximum output power (0 dBm). Assuming a digital canceler at the radio back-end provides a TX SI attenuation of 40dB [4] and further assuming the TX-to-RX isolation provided by either a circulator or two-antennas is 20dB, the leaves an additional 30dB cancellation required in the analog/RF domain, see Fig. 1. This work explores a low-noise, low-power feedforward RF SI cancellation technique and a switch-mode PA method which minimizes unwanted TX spurious output, Fig. 1.

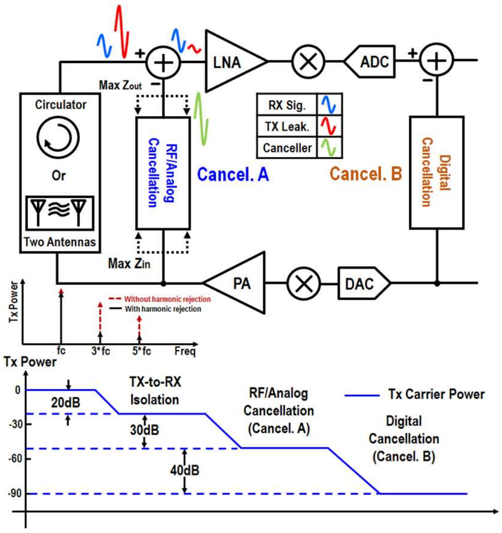

Fig. 1 Conceptual diagram and system analysis of the proposed TX SI cancellation and harmonic-rejection front-end.

The paper is organized as follows: Section II describes the proposed polyphase-filter based SI canceler, Section III presents the circuit implementation details, while Section IV provides measurement results, followed by concluding comments in Section V.

II. SI Cancellation Method and Harmonic-Rejection Power Amplifier

The front-end air interface provides an isolation of 20-30dB with an arbitrary phase. Thus, the SI canceler needs to be designed with a maximum gain of -20dB as well as a 360º phase rotation. Any cancellation method must be designed without degrading the standalone performance of the TX and RX – e.g. no degradation of the RX NF, lowering the TX efficiency, etc.

A. SI Cancellation Approach

This SI cancellation circuitry uses a polyphase filter (PPF) and tunable G_m stages to achieve a 360º phase rotation with a gain tuning range from -40 to -20 dB. This allows proper tracking (phase and amplitude) of the TX SI which couples back into the RX, see Fig. 3.

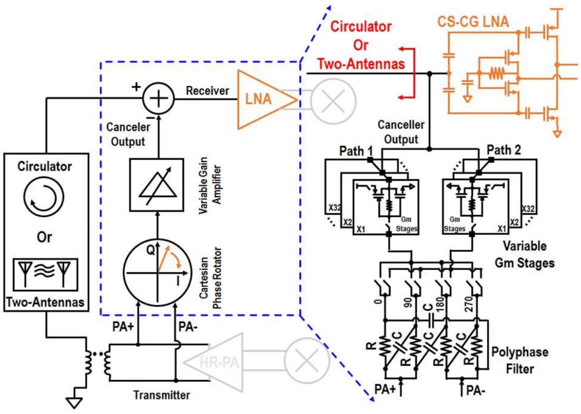

Fig. 3 Polyphaser filter (PPF) based Cartesian canceler schematic.

This self-interference feedforward canceler is connected between the PA output and the LNA input. This canceler utilizes a PPF to generate roughly four equal amplitude signals with a phase difference of 0º, 90º, 180º and 270º, see Fig. 3. The canceler phase and gain tuning is performed by first selecting two of the four phases at the PPF output. These two signals which have an approximate 90º phase difference, are each weighted using variable gain transconductance stages. The two outputs are combined, to produce a vector sum which is equal in amplitude and phase to the leakage signal. This approach effectively applies a Cartesian rotator to the cancellation path by generating a vector signal copy of the TX-leakage signal.

To reduce the effect of loading on both the PA output and LNA input matching network, the canceler input and output impedances are greater than 900Ω and 500Ω, respectively. Adding active devices at the RX input usually introduces a non-negligible noise figure (NF) degradation. However, the front-end leakage media will attenuate the SI signal by at least 20dB. Thus, any active circuitry in the cancellation path must attenuate the signal by an equal amount (20dB) to match the leakage magnitude. The canceler output is a current-mode signal generated by a set of low-power G_m stages which consume less than 0.3mA. Compared to prior transformer-based cancelers [6], this cancellation circuit requires significantly less die area. In addition, the noise injected into the RX path, from the canceler, is minimized by two features: 1) the cancellation path maximum gain is -20dB, 2) the required low gain of the G_m stage is exploited to increase the equivalent noise resistance (250Ω) looking into the canceler output. From the perspective of the RX point of injection, equivalent noise resistance is comparatively higher, as desired, than the 50Ω radiation impedance of the antenna. Thus, the canceler contribution to the RX NF is near negligible, less than 0.6dB.

B. Harmonic-Rejection Power Amplifier

To reduce the power amplifier output harmonics, the PA combines three parallel driver stages with a relative phase difference of 0º, 45º, 90º, and gain ratios of 1, $\sqrt{2}$, 1, respectively, see Fig. 2. This approach effectively realizes a stair-like function, as was similarly done in [12] for a mixer. An alternate singled-ended version of this HRPA, which cancels the second harmonic, was published in [13]. The proposed HRPA obviates the need for discrete external components in moderate output power applications (e.g. Bluetooth).

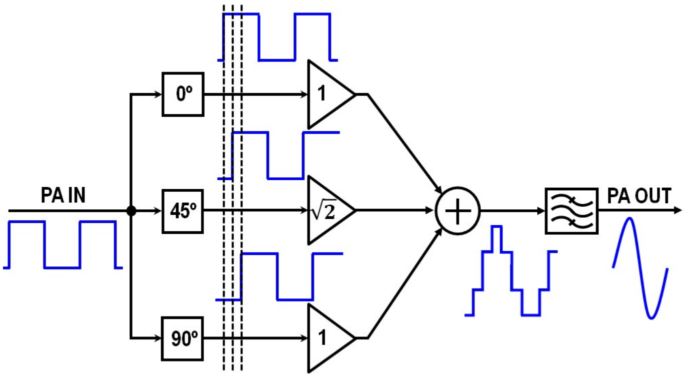

Fig. 2 Architecture of the proposed harmonic-rejection power amplifier.

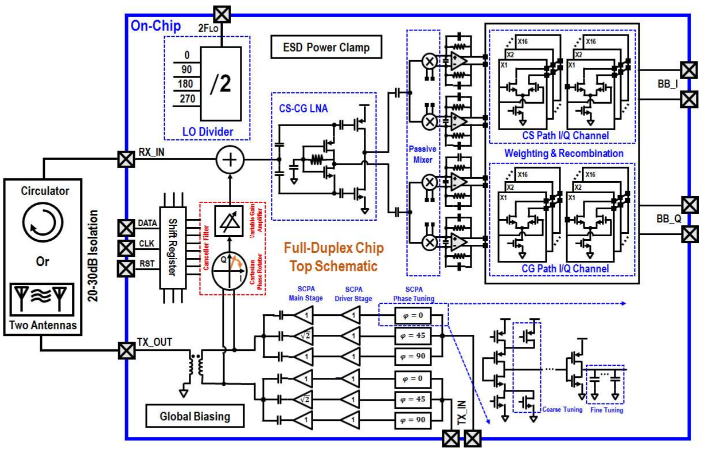

Fig. 4 Detailed block diagram of the full-duplex front-end with low-noise same-channel self-interference cancellation and HRPA.

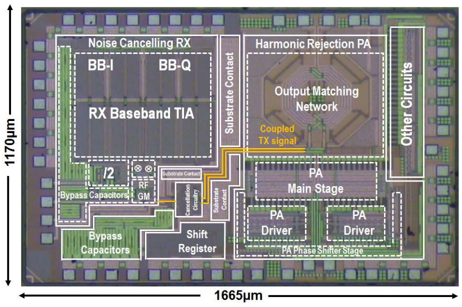

Fig. 5 TSMC 40nm die micrograph of full-duplex transceiver.

III. Circuit Implementations

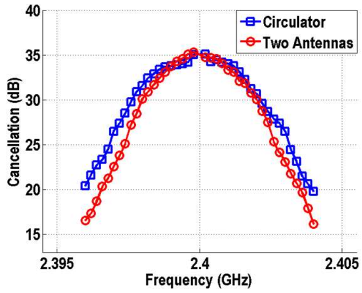

Fig. 6 Measurement results of TX leakage suppression versus bandwidth using both a circulator and two antennas.

As a demonstration of the proposed SI canceler system, a transceiver front-end is designed to have performance similar to that of a Bluetooth radio, with the exception of enabling an FD feature, Fig. 4. The differential input of the SI canceler is attached to the primary side of the TX output transformer, to provide SI cancellation at the LNA input. A switch-capacitor PA (SCPA) is implemented with a harmonic-reject feature. The RX utilizes a noise-canceling current-mode architecture to improve the out-of-band linearity. An integrated divide-by-two circuit generates a 25% duty cycle LO which drives the mixers.

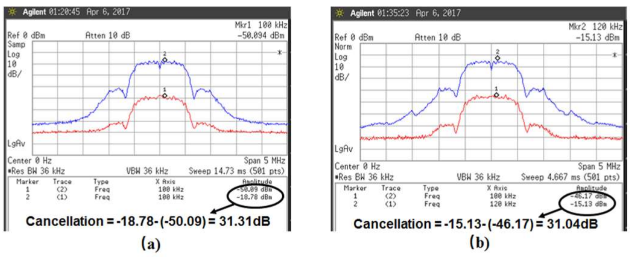

Fig. 7 Measured TX suppression using a modulated GFSK signal. Baseband output spectrum with cancellation enabled/disabled, (a) measurement with a circulator, (b) measurement with two antennas.

IV. Measurement Results

This chip is fabricated in a TSMC 40nm CMOS process with a six-layer metal stack and a UTM layer. The die is assembled with the test-board using chip-on-board packaging. A die photo is shown in Fig. 5. The self-interference cancellation circuitry is compact and occupies an area of less than 131μm × 112.5μm.

The RX operates from 1 to 3 GHz with a measured gain of 45dB, a 1.5MHz 3dB channel BW, a 4.5 dB in-band noise figure, an 18 dBm out-of-band IIP_3 and an 8.5 dBm out-of-band input P_{-1dB}. The RX consumes 10mA from a 1.1 V supply which includes 4mA from the LNA stage, 0.7mA from each of the four baseband operational amplifiers and 3mA for the LO dividers.

All SI cancellation measurements were performed using two different front-end air interface solutions, a circulator and two antennas. Both media have a measured TX-to-RX isolation of 20-30dB. The integrated PA delivers an output power of 0dBm while the SI cancellation measurements are performed. A maximum cancellation of 35dB was measured and a 30dB cancellation was achieved over a 4 MHz BW, Fig. 6. The SI cancellation was repeated with GFSK modulated signal, Fig. 7.

RX noise figure measurements were performed to characterize the canceler network, using a desired RX signal 100 kHz offset frequency from the TX signal. After the canceler is enabled, the RX NF degradation is 0.6dB, see Fig. 8.

The HR SCPA was measured with both single-tone and modulated signals. The PA has a measured +14 dBm maximum output power with a 33% drain efficiency. The measured HRPA reduction of the 3^{rd} and 5^{th} harmonics (Fig. 9) are 30dB and 15dB, respectively. Using a GFSK modulated input signal with the PA set to maximum output power, a 0.6% EVM was measured.

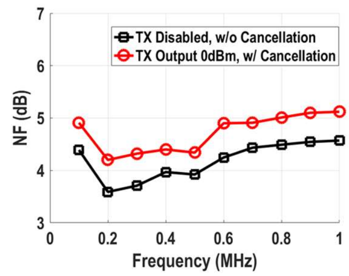

Fig. 8 Measured RX noise figure with 0 dBm PA output with the canceler enabled and disabled, relative to the baseband frequency.

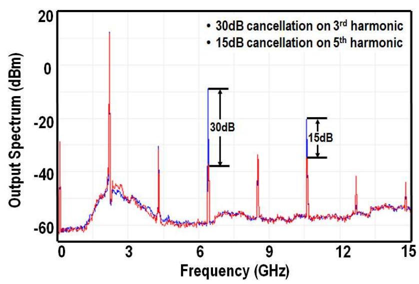

Fig. 9 Measured PA output spectrum with harmonic rejection enabled and disabled.

Table I: Comparison Table

SI Cancellation		J. Zhou' 2015 ISSCC	Van Den Broek' 2015 ISSCC	D. Yang' 2015 JSSC	N. Reiskarimian' 2017 ISSCC	T. Zhang' 2017 ISSCC	This Work
Architecture		FD Equalization	VM-Downmixer	BB Duplexing LNA	Magnetic-Free Circulator Receiver	Dual Path + Adaptive Filter	Polyphase Filter + Active Gm Stage
Technology		65nm	65nm	65nm	65nm	40nm	40nm
Cancellation BW	Cancellation(dB)	20	27	33	40[2]	50	30
	BW(MHz)	15/25[1]	16.25	0.3	20	42	4
RX NF degradation due to TX SI cancellation (dB)		0.9-1.2/ 1.1-1.5[1]	4-6	N/A	1.7	1.5	*0.6*
Max TX port operating power (dBm)		N/A	N/A	-17.3	8	15	0
Canceler IIP3 (dBm)		N/A	N/A	N/A	N/A[3]	36	15
Canceller power (mW)		44-91	N/A	N/A	36	11.5	*0.25*
Canceller area (µm2)		N/A	N/A	N/A	N/A	203×124(RF)+ 925×350(BB)	*131×112.5*

[1]Measurement taken with an antenna pair. 15MHz BW, 0.9-1.2dB NF degradation is with one filter. 25MHz, 1.1-1.5dB is with two filters. [2]Digital SI cancellation is not included. [3]Measured TX-Antenna IIP_3 is 30dBm.

TX Harmonic Rejection	T. Sano' 2015 ISSCC	A. Ba' 2014 RFIC	This Work
Architecture	Conduction Angle Calibration	Conduction Angle Calibration	HR SCPA
Technology	40nm	40nm	40nm
Output Power (dBm)	0	1.2	14
Drain Efficiency (%)	-NA-	39	30
Off-chip Matching network	No	Yes	No
HD3 (dBc)	-48	<-50	-22.6 (before) /-51.9 (after)
HD5 (dBc)	-NA-	<-50	-31 (before) /-45.3 (after)
EVM (%)	-NA-	-NA-	0.6

A performance comparison is given in Table I. The measurement results from this prototype chip demonstrates promise toward Bluetooth-like applications using FD radios.

V. Conclusions

This paper introduces several methods to enable TX SI cancellation and TX output harmonic rejection for low-power FD radios. This effort describes a low-noise, low-power SI cancellation technique and a HRPA which contribute toward reducing the interaction between the TX and RX in the analog front-end, to eventually realize FD radios.

Acknowledgment

This work is supported by NSF 1408575, Marvell Ltd, and CDADIC.

References

[1] J. Zhou, T. H. Chuang, T. Dinc, and H. Krishnaswamy, "Receiver with >20MHz bandwidth self-interference cancellation suitable for FDD, co-existence and full-duplex applications," in *IEEE Int. Solid-State Circuits Conf. (ISSCC) Dig. Tech. Papers*, 2015, pp. 1–3.

[2] D. Yang, H. Yuksel, and A. Molnar, "A Wideband Highly Integrated and Widely Tunable Transceiver for In-Band Full-Duplex Communication," *IEEE J. Solid-State Circuits*, vol. 50, no. 5, pp. 1189–1202, May 2015.

[3] D. J. van den Broek, E. A. M. Klumperink, and B. Nauta, "A self-interference-cancelling receiver for in-band full-duplex wireless with low distortion under cancellation of strong TX leakage," in *2015 IEEE International Solid-State Circuits Conference - (ISSCC) Digest of Technical Papers*, 2015, pp. 1–3.

[4] N. Reiskarimian, M. B. Dastjerdi, J. Zhou, and H. Krishnaswamy, "Highly-linear integrated magnetic-free circulator-receiver for full-duplex wireless," in *2017 IEEE International Solid-State Circuits Conference (ISSCC)*, 2017, pp. 316–317.

[5] T. Zhang, A. Najafi, C. Su, and J. C. Rudell, "A 1.7-to-2.2GHz Full-Duplex Transceiver System with >50dB Self-Interference Cancellation over 42MHz Bandwidth," in *IEEE Int. Solid-State Circuits Conf. (ISSCC) Dig. Tech. Papers*, 2017, pp. 314–315.

[6] T. Zhang, A. R. Suvarna, V. Bhagavatula, and J. C. Rudell, "An Integrated CMOS Passive Self-Interference Mitigation Technique for FDD Radios," *IEEE J. Solid-State Circuits*, vol. 50, no. 5, pp. 1176–1188, May 2015.

[7] T. Zhang, A. R. Suvarna, V. Bhagavatula, and J. C. Rudell, "An integrated CMOS passive transmitter leakage suppression technique for FDD Radios," in *IEEE Radio Freq. Integr. Circuits (RFIC) Symp.*, 2014, pp. 43–46.

[8] S. Ramakrishnan, L. Calderin, A. Puglielli, E. Alon, A. Niknejad, and B. Nikolić, "A 65nm CMOS transceiver with integrated active cancellation supporting FDD from 1GHz to 1.8GHz at +12.6dBm TX power leakage," in *2016 IEEE Symposium on VLSI Circuits (VLSI-Circuits)*, 2016, pp. 1–2.

[9] T. Sano *et al.*, "A 6.3mW BLE transceiver embedded RX image-rejection filter and TX harmonic-suppression filter reusing on-chip matching network," in *IEEE Int. Solid-State Circuits Conf. (ISSCC) Dig. Tech. Papers*, 2015, pp. 1–3.

[10] A. Ba, V. K. Chillara, Y.-H. Liu, H. Kato, K. Philips, and R. B. Staszewski, "A 2.4GHz class-D power amplifier with conduction angle calibration for –50dBc harmonic emissions," in *IEEE Radio Freq. Integr. Circuits (RFIC) Symp.*, 2014, pp. 239–242.

[11] C.-W. Tang, "Harmonic-suppression LTCC filter with the step-impedance quarter-wavelength open stub," *IEEE Trans. Microw. Theory Tech.*, vol. 52, no. 2, pp. 617–624, Feb. 2004.

[12] J. A. Weldon *et al.*, "A 1.75 GHz highly-integrated narrow-band CMOS transmitter with harmonic-rejection mixers," in *IEEE Int. Solid-State Circuits Conf. (ISSCC) Dig. Tech. Papers*, 2001, pp. 160–161.

[13] C. Huang, Y. Chen, T. Zhang, V. Sathe, and J. C. Rudell, "A 40nm CMOS single-ended switch-capacitor harmonic-rejection power amplifier for ZigBee applications," in *2016 IEEE Radio Frequency Integrated Circuits Symposium (RFIC)*, 2016, pp. 214–217.